




## RESEARCH ARTICLE

# Optimal gamma-band entrainment of visual cortex

Nathan M. Petro<sup>1</sup>  | Lauren K. Webert<sup>1</sup>  | Seth D. Springer<sup>1,2</sup> |  
Hannah J. Okelberry<sup>1</sup> | Jason A. John<sup>1</sup> | Lucy K. Horne<sup>1</sup> | Ryan Glesinger<sup>1</sup> |  
Maggie P. Rempe<sup>1,2</sup> | Tony W. Wilson<sup>1,2,3</sup> 

<sup>1</sup>Institute for Human Neuroscience, Boys Town National Research Hospital, Boys Town, Nebraska, USA

<sup>2</sup>College of Medicine, University of Nebraska Medical Center (UNMC), Omaha, Nebraska, USA

<sup>3</sup>Department of Pharmacology and Neuroscience, Creighton University, Omaha, Nebraska, USA

## Correspondence

Nathan M. Petro, Postdoctoral Research Fellow, Institute for Human Neuroscience, Boys Town National Research Hospital, Boys Town, NE, USA.

Email: [nathan.petro@boystown.org](mailto:nathan.petro@boystown.org)

## Funding information

National Institutes of Health, Grant/Award Numbers: R01-MH116782, R01-MH118013, S10-OD028751, R01-DA047828, R01-DA056223, P20-GM144641, F30-AG076259

## Abstract

Visual entrainment is a powerful and widely used research tool to study visual information processing in the brain. While many entrainment studies have focused on frequencies around 14–16 Hz, there is renewed interest in understanding visual entrainment at higher frequencies (e.g., gamma-band entrainment). Notably, recent groundbreaking studies have demonstrated that gamma-band visual entrainment at 40 Hz may have therapeutic effects in the context of Alzheimer's disease (AD) by stimulating specific neural ensembles, which utilize GABAergic signaling. Despite such promising findings, few studies have investigated the optimal parameters for gamma-band visual entrainment. Herein, we examined whether visual stimulation at 32, 40, or 48 Hz produces optimal visual entrainment responses using high-density magnetoencephalography (MEG). Our results indicated strong entrainment responses localizing to the primary visual cortex in each condition. Entrainment responses were stronger for 32 and 40 Hz relative to 48 Hz, indicating more robust synchronization of neural ensembles at these lower gamma-band frequencies. In addition, 32 and 40 Hz entrainment responses showed typical patterns of habituation across trials, but this effect was absent for 48 Hz. Finally, connectivity between visual cortex and parietal and prefrontal cortices tended to be strongest for 40 relative to 32 and 48 Hz entrainment. These results suggest that neural ensembles in the visual cortex may resonate at around 32 and 40 Hz and thus entrain more readily to photic stimulation at these frequencies. Emerging AD therapies, which have focused on 40 Hz entrainment to date, may be more effective at lower relative to higher gamma frequencies, although additional work in clinical populations is needed to confirm these findings.

This is an open access article under the terms of the [Creative Commons Attribution-NonCommercial-NoDerivs](https://creativecommons.org/licenses/by-nc-nd/4.0/) License, which permits use and distribution in any medium, provided the original work is properly cited, the use is non-commercial and no modifications or adaptations are made.

© 2024 The Author(s). *Human Brain Mapping* published by Wiley Periodicals LLC.

### Practitioner Points

- Gamma-band visual entrainment has emerged as a therapeutic approach for eliminating amyloid in Alzheimer's disease, but its optimal parameters are unknown.
- We found stronger entrainment at 32 and 40 Hz compared to 48 Hz, suggesting neural ensembles prefer to resonate around these relatively lower gamma-band frequencies.
- These findings may inform the development and refinement of innovative AD therapies and the study of GABAergic visual cortical functions.

### KEYWORDS

gamma activity, magnetoencephalography, MEG, visual entrainment

## 1 | INTRODUCTION

Visual entrainment is a phenomenon whereby neural populations in the visual cortex synchronize their firing to an external stimulus (e.g., a flickering light). This visual entrainment response is distinct from a transient response (Notbohm et al., 2016), where the onset of a stimulus evokes a single instance of synchronized neural activity (Regan, 1989). The amplitude of visual entrainment responses are thought to reflect the overall size of the neural population locked to the photic stimulation (Di Russo et al., 2007; Hillyard et al., 1997; Lopes da Silva, 1991; Pfurtscheller & Lopes da Silva, 1999), with many studies showing aberrant visual entrainment amplitudes in the context of neurological and psychiatric disorders (Angelini et al., 2004; Clementz et al., 2004; Jin et al., 2000; Shibata et al., 2008; Springer et al., 2022), as well as modulation by transcranial brain stimulation techniques (Heinrichs-Graham et al., 2017). More broadly, studies have shown that visual entrainment is a powerful research tool for studying the integrity of neural ensembles and may be sensitive to some of the earliest signs of neuropathology.

While the majority of previous work has focused on entrainment in the canonical alpha and beta frequency bands (< 20 Hz), interest in visual entrainment at higher frequencies (i.e., gamma range) has recently increased. Converging evidence from multiple studies indicates that entrainment at around the alpha (~10 Hz) and low beta (~15 Hz) frequencies tend to elicit the strongest and most robust visuocortical response relative to neighboring frequencies (Herrmann, 2001; Lazarev et al., 2001; Pastor et al., 2003, 2007). This spectral preference or advantage may reflect that local neural ensembles in the visual cortex tend to endogenously resonate within this frequency range (Pastor et al., 2003). However, as noted above, visual entrainment at higher frequencies (i.e., gamma range) has been far less studied, despite the recent increase in interest due to potential therapeutic interventions in the context of Alzheimer's disease (AD). Specifically, groundbreaking animal studies have demonstrated that visual entrainment in the gamma band can reduce amyloid- $\beta$  and hyperphosphorylated tau in the brain (Adaikkan et al., 2019; Hu et al., 2023; Iaccarino et al., 2016;

Martorell et al., 2019). This animal work has led to nascent human studies, where sessions of 40 Hz photic stimulation have been tentatively linked to a reduction in the clinical manifestations (Cimenser et al., 2021; Clements-Cortes et al., 2016) and biomarkers of AD (Chan et al., 2022; He et al., 2021) in some patients (for reviews, see Hu et al., 2023; Manippa et al., 2022; Traikapi & Konstantinou, 2021). Unfortunately, the two studies that directly measured levels of amyloid- $\beta$  (and hyperphosphorylated tau) in humans found no changes following 40 Hz photic stimulation therapy (He et al., 2021; Ismail et al., 2018). Similarly mixed results have been found when stimulating the frontal or precuneus cortex at 40 Hz using transcranial alternating current stimulation (tACS; (Benussi et al., 2021, 2022; Dhaynaut et al., 2022; Kehler et al., 2020; Kim et al., 2021; Moussavi et al., 2021; Naro et al., 2016; Zhou et al., 2022; but see Sprugnoli et al., 2021)) or repetitive transcranial magnetic stimulation (rTMS; (Koch et al., 2022)). While intriguing, gamma-band entrainment therapy in humans has yet to show the same promise as in animal models.

The discrepancy between the animal and human studies could be species related differences in the ideal parameters for gamma-band visual entrainment. In other words, while 40 Hz entrainment produces the strongest entrainment in rodents, a different gamma-band frequency may be better suited for entrainment in the human brain. For instance, some studies have shown that lower gamma-band frequencies (30 to 35 Hz) compared to 40 Hz photic stimulation elicits the stronger entrainment (Lee et al., 2021; Park et al., 2022; Pastor et al., 2003), while other studies have shown an advantage at higher frequencies (~47 Hz; (Gulbinaite et al., 2019)). Moreover, a recent study demonstrated improved memory recall in healthy adults following gamma-band entrainment at frequencies above 40 Hz (i.e., 60 Hz; (Manippa, Filardi, et al., 2024)). Importantly, the therapeutic effects in animals are strongest in neural tissues that strongly entrain to the photic stimulation (Iaccarino et al., 2016; Martorell et al., 2019). Thus, entraining tissue more strongly and/or entraining a larger area of neural tissue would likely improve therapeutic outcomes, pointing to a need to identify the optimal parameters for gamma-band visual entrainment.

In addition to its newfound therapeutic relevance, gamma band activity has long been a characteristic of efficient neural processing. In the visual cortex, gamma band activity is thought to support the binding of low-level visual information into coherent objects in perception (Fries et al., 2001; Keil et al., 1999; Tallon-Baudry & Bertrand, 1999). More generally, gamma activity across the brain is crucial to the efficiency of neural information processing (Uhlhaas et al., 2009) that is essential for cognitive processes (Jensen et al., 2007; Tallon-Baudry, 2009; Uhlhaas & Singer, 2006). Along these lines, gamma activity is aberrant in disorders where cognition is impaired (Arif et al., 2020; Casagrande et al., 2022; Groff et al., 2020; Kocagoncu et al., 2020; Spooner et al., 2018; Uhlhaas & Singer, 2006; Wiesman et al., 2018; Wilson et al., 2011), including AD (Güntekin et al., 2013; Jafari et al., 2020; Meehan et al., 2023; Stam et al., 2002; Wiesman, Murman, et al., 2021) and HIV-related cognitive decline (Casagrande et al., 2021; Spooner et al., 2018, 2020; Wilson et al., 2016, 2019). Gamma activity is thought to arise from local neural ensembles involving GABAergic communication (Buzsáki & Wang, 2012; Kujala et al., 2015; Wilson et al., 2018). In fact, recent work using MR-spectroscopy has linked GABA concentration to gamma activity (Balz et al., 2016; Chen et al., 2014; Edden et al., 2009; Gaetz et al., 2011; Muthukumaraswamy et al., 2009), and GABA signaling is disrupted in disorders with aberrant gamma activity (Bi et al., 2020; Chen et al., 2014; Enomoto et al., 2011; Jiménez-Balado & Eich, 2021; Rissman et al., 2007; Rissman & Mobley, 2011; Wilson et al., 2007). Thus, identifying the precise gamma frequencies that produce the strongest visual entrainment responses may have important therapeutic implications in the context of neurology and psychiatry, and may advance the field's understanding of many aspects of visual perception and the role of local GABA-gated circuitry.

In the current study, we examined whether visual stimulation at a specific gamma-band frequency is optimal for visual entrainment. As noted above, recent therapeutic approaches to AD have focused on 40 Hz entrainment, but whether this frequency is optimal for gamma range visual entrainment in humans is unknown. Thus, we focused on gamma entrainment at equal increments around this 40 Hz frequency (32 Hz, 40 Hz, and 48 Hz) to determine whether entrainment would be stronger at slower or faster gamma band frequencies. These frequencies were specifically chosen in order to include a lower bound of the gamma band that is near beta, as well as a higher gamma frequency that is equidistant from 40 Hz. We limited the conditions to three to ensure task compliance and limit participant fatigue, as the experiment was about 15 minutes long with the three current conditions. In addition to entrainment amplitude, we tested whether the different stimulation frequencies were associated with distinct habituation patterns across trials (Abdulhussein et al., 2022; Megela & Teyler, 1979; Rauschel et al., 2016; Schupp et al., 2006) and/or different whole-brain functional connectivity patterns with the visual cortices. Our primary hypotheses were that all frequencies would lead to robust gamma entrainment in primary visual cortices, but that the three stimulation frequencies would be associated with significant differences in entrainment amplitude, potentially reflecting the ideal resonant frequency of local GABA circuits.

## 2 | METHODS

### 2.1 | Participants

A total of 28 adults (11 males, 17 females) with a mean age of 26.14 (SD = 4.31) years were selected for inclusion in this study. Of the 28 adults, 7.14% were left-handed, 14.28% were Black, 3.57% were American Indian/Alaska Native, 75.00% were Caucasian, and 7.14% were more than one race. This distribution corresponds closely to the racial demographics of the surrounding area. Exclusionary criteria included any medical illness affecting CNS function (e.g., HIV/AIDS, Lupus, etc.), any neurological or psychiatric disorder, cognitive impairment, history of head trauma, current substance abuse, and the standard exclusionary criteria related to MEG and MRI acquisition (e.g., ferromagnetic implants). The Institutional Review Board reviewed and approved this investigation. Each participant provided written informed consent following a detailed description of the study.

### 2.2 | Experimental paradigm

During the MEG recording, participants sat in a nonmagnetic chair within a magnetically shielded room and were instructed to fixate on an entrainment stimulus that flickered at 32, 40, or 48 times per second (Hz) with a 50% duty-cycle. The stimulus was a small white circle, 2.75 inches in diameter that was presented centrally on a black background and subtended a visual angle of 3.5°. The duration of each flicker-train was 1500 ms and the interstimulus interval was a random interval between 2000 and 2500 ms (Figure 1). The order of flicker frequencies (i.e., 32 Hz, 40 Hz, and 48 Hz) was pseudorandomized so that no more than three trials of the same frequency were presented consecutively. Participants completed 74 trials per flicker frequency, resulting in 222 total trials. The entrainment stimuli were presented using the Psychophysics Toolbox (Kleiner et al., 2007) and a PROPixx DLP LED projector (VPixx Technologies Inc., Saint-Bruno-de-Montarville, Canada). The stimulation frequencies were verified using a fast Fourier transform of data from a fiber-optic photodiode attached to the presentation screen while the experimental paradigm was displayed. To ensure that participants were attending to the flickering stimulus, the task had 24 oddball trials in which participants were instructed to respond via button press with their right index finger when the fixation dot changed from grey to blue. A total of 246 trials were completed, for a total run time of 15.5 minutes.

### 2.3 | MEG data acquisition

All MEG recordings were conducted in a two-layer magnetically-shielded VACOSHIELD room (Vacuumschmelze, Hanau, Germany). Neuromagnetic responses were sampled continuously at 1 kHz, with an acquisition bandwidth of 0.1–330 Hz, using a MEGIN Triux Neo MEG system with 306 magnetic sensors (Helsinki, Finland). During

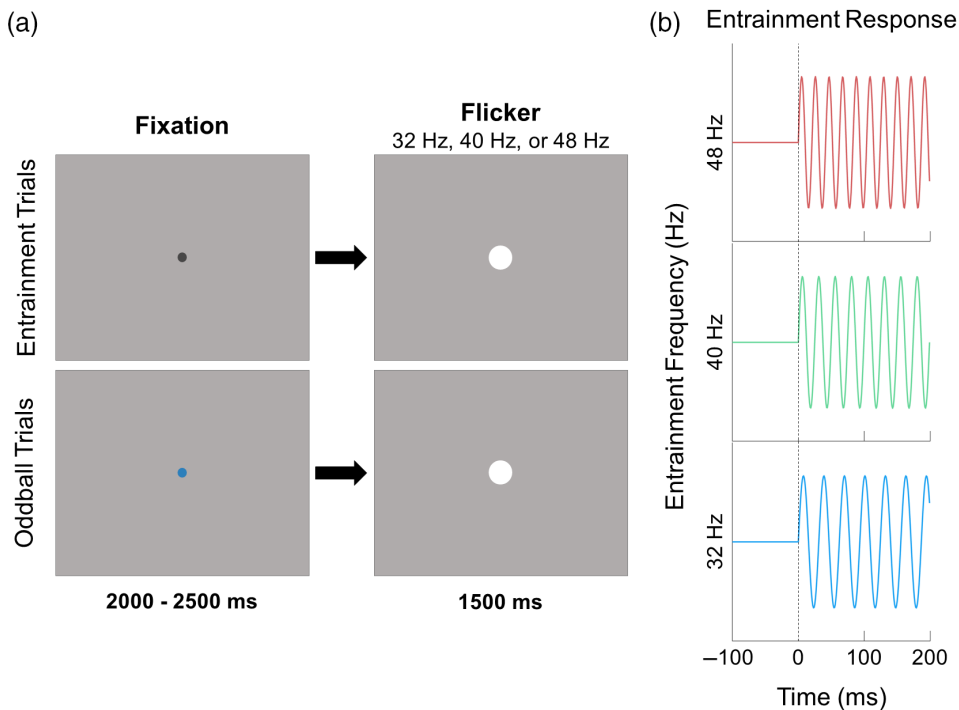


**FIGURE 1** Schematic of entrainment task design. (a) A white dot was presented on a gray background and flickered on-and-off at either 32 Hz, 40 Hz, or 48 Hz. Each trial was preceded by a fixation dot that was either black (80% of trials) or blue (20% of trials); participants were instructed to respond to the blue dot with a button press made with the index finger. The blue dot trials were excluded from further analysis. (b) Sine waves illustrating entrainment patterns for each of the three frequencies.

data acquisition, participants were monitored via real-time audiovisual feeds from inside the shielded room. Subject-wise MEG data were corrected for head motion and subjected to external noise reduction using signal space separation with a temporal extension (Taulu & Simola, 2006).

## 2.4 | Structural MRI processing, and MEG coregistration

Preceding MEG measurement, five head position indicator (HPI) coils were attached to the participant's head and localized, together with three fiducial points and at least 100 scalp surface points, with a 3D digitizer (Fastrak, Polhemus Navigator Sciences, Colchester, VT, USA). Once in the MEG, electrical currents with unique frequencies (e.g., 322 Hz) were fed into each of the HPI coils. These HPI coil currents induced measurable magnetic fields, allowing the position of the HPI coils to be actively tracked relative to the MEG sensors throughout the recording. Since HPI coil locations are known in head coordinates, all MEG measurements could be transformed into a common coordinate system. With this coordinate system, subject-wise MEG data were coregistered with their high-resolution structural T1-weighted MRI data prior to source reconstruction using BESA MRI (Version 3.0, BESA GmbH, Gräfelfing, Germany). Structural MRI data were transformed into standardized space and aligned parallel to the anterior and posterior commissures. Following source analysis, each participant's MEG functional images were also transformed into standardized space and spatially resampled to enable comparison across participants.

## 2.5 | MEG preprocessing, time-frequency transformation, and sensor-level statistics

Cardiac and ocular artefacts (blinks and eye movements) were removed from the data using signal-space projection (SSP), which was accounted for during source analysis (Uusitalo & Ilmoniemi, 1997). The continuous magnetic time series was divided into 3500 ms epochs, with the baseline period being defined as the 600 ms prior to the onset of the flickering stimulus (i.e.,  $-600$  to  $0$  ms). Subsequently, epochs with remaining artifacts (after cardiac and ocular artifact correction) were removed based on a fixed threshold method, supplemented with visual inspection. Briefly, the amplitude and gradient distributions across all trials were determined per participant, and those trials containing the highest amplitude and/or gradient values relative to this distribution were rejected based on participant-specific thresholds. This approach was employed to minimize the impact of individual differences in sensor proximity to the brain and overall head size, which strongly affect MEG signal amplitude. Artifact-free epochs were then transformed into the time-frequency domain using complex demodulation (Hochstetter et al., 2004; Kovach & Gander, 2016; Papp & Ktonas, 1977), with a resolution of 0.5 Hz and 100 ms between 2 and 100 Hz. Following time-frequency transformation, spectral power estimates per sensor were averaged across trials to generate plots of mean spectral density per sensor. These sensor-level data were then normalized to the baseline power within each frequency bin, which was calculated as the mean power for that 0.5 Hz bin during the  $-600$  to  $0$  ms time period.

The significant time-frequency windows used for source imaging were determined by statistical analysis of the sensor-level

spectrograms across the entire array of 204 gradiometers conducted in BESA Statistics (Version 2.1 T, BESA GmbH, Gräfelting, Germany). Briefly, each pixel per spectrogram was initially evaluated using a mass univariate approach based on the general linear model, followed by cluster-based permutation testing to address the problem of multiple comparisons (Ernst, 2004; Maris & Oostenveld, 2007). Specifically, a two-stage procedure was utilized to minimize false positive results while maintaining sensitivity. The first stage consisted of performing paired-sample *t*-tests against baseline on each pixel per spectrogram and thresholding the output spectrograms of *t*-values at  $p < .05$  to define time-frequency bins containing potentially significant oscillatory deviations from baseline. Time-frequency bins that survived thresholding (at  $p < .05$ ) were clustered with temporally and/or spectrally neighboring bins that also survived, and cluster values were derived by summing all *t*-values within each cluster. In stage two, non-parametric permutation testing was used to derive a distribution of cluster-values and the significance level of the cluster(s) from stage one were tested directly using this permuted distribution, which was the result of 10,000 permutations. Based on this cluster-based permutation analysis, only the time-frequency windows that contained significant oscillatory deviations from baseline at the  $p < .001$ , corrected, threshold across all participants were subjected to source imaging (i.e., beamforming).

## 2.6 | MEG source imaging and statistics

Cortical regions were imaged through a time-frequency-resolved extension of the linearly constrained minimum variance (LCMV) beamformer (Dalal et al., 2006; Gross et al., 2001; Van Veen et al., 1997). The images were derived from the cross spectral densities of all combinations of MEG gradiometers averaged over the time-frequency range of interest, and the solution of the forward problem for each location on a grid specified by input voxel space. In principle, the beamformer operator generates a spatial filter for each grid point that passes signals without attenuation from a given neural region, while suppressing activity in all other brain areas. The filter properties arise from the forward solution (i.e., lead field matrix) for each location on a volumetric grid specified by input voxel space and from the MEG cross spectral density matrix. Basically, for each voxel, a set of beamformer weights is determined, which amounts to each MEG sensor being allocated a sensitivity weighting for activity in the particular voxel. Following convention, the source power in these images was normalized per participant using a pre-stimulus period (i.e., baseline) of equal duration and bandwidth (Hillebrand et al., 2005). Such images are typically referred to as pseudo-*t* maps, with units (pseudo-*t*) that reflect noise-normalized power differences (i.e., active vs. passive) per voxel. MEG pre-processing and imaging used the Brain Electrical Source Analysis (version 7.1) software.

To assess the anatomical basis of the responses identified through the sensor-level analysis, the 3D beamformer output maps were

averaged across all participants. To investigate neural differences in visual processing as a function of stimulation frequency, virtual sensors were extracted per participant from the voxel with the strongest entrainment response per hemisphere in the grand-averaged image (i.e., across all participants and conditions). To compute virtual sensors (i.e., voxel time series data), we applied the sensor weighting matrix derived from the forward solution to the preprocessed signal vector, which yielded a time series for the specific voxels in source space. For each coordinate of interest, the envelope of spectral power was computed for the frequency range used in the beamforming analysis, which was centered around each entrainment frequency (i.e., 31–33 Hz, 39–41 Hz, and 47–49 Hz; see below). For each participant, the mean baseline activity per spectral window (e.g., 31–33 Hz) was derived by averaging the absolute amplitude time series data across the baseline period (–500 to 0 ms). This value was then used to normalize the post-stimulus time series. Estimates of the entrainment response were derived by averaging these normalized time series across the time window used in the beamforming analyses (i.e., 500 to 1000 ms; see below). Since we did not have any laterality hypotheses, we collapsed across hemispheres for each spectral window.

## 2.7 | Statistical analyses: Effect of entrainment frequency on oscillatory power

The effect of entrainment frequency (i.e., 32 Hz, 40 Hz, and 48 Hz) on oscillatory power was tested using repeated measures analysis of variance (ANOVA) implemented in IBM SPSS Statistics (Version 25). This model included oscillatory power for each frequency, with a within subjects factor of entrainment frequency that had three levels. Finally, to reduce the impact of outliers on statistical analyses, participants with values 2.5 SDs above or below the group mean were excluded for each analysis. In total, three participants were excluded for outlying data. Note that including or excluding these participants did not change our significant findings.

## 2.8 | Statistical analysis: Habituation of entrainment response

To determine if the entrainment responses showed a habituation pattern, the single trial values of oscillatory power were submitted to a linear mixed-effects model using the *nlme* package (Pinheiro et al., 2022; Pinheiro & Bates, 2000) in R, where oscillatory power was compared to trial number across all participants. Specifically, the model was implemented as:  $\text{Power} \sim \text{Frequency} \times \text{Trial}$ ,  $\text{random} = (\sim 1 + \text{Frequency} | \text{Participant})$ , assuming a normal Gaussian distribution of random effects. In addition to investigating the overall effect of habituation, we investigated the simple slopes of each frequency to determine which entrainment frequencies habituate across trials.

## 2.9 | Functional connectivity

To investigate how cortico-cortico interactions differ as a function of entrainment frequency, the peak voxels from the primary visual cortex in the statistical maps described above were used as seeds for calculation of a coherence beamformer using the dynamic imaging of coherent signals (DICS) approach (Gross et al., 2001). Briefly, this approach uses the time-frequency averaged cross-spectral density to calculate voxel-wise estimates of neural coherence (i.e., connectivity). These whole-brain images represent the voxel-wise coherence with the identified reference or seed voxel. One whole-brain image per entrainment frequency was calculated using the left and right visual cortical seed separately, and then averaged together per participant and entrainment frequency. Note that eight participants were excluded from this analysis as their connectivity values contained outlying data. Because oscillatory power can artificially inflate estimates of connectivity (Schoffelen & Gross, 2009), we covaried out oscillatory amplitude from these connectivity maps. These connectivity maps were examined using a voxel-wise repeated measures ANOVA, with a single within-subjects factor of entrainment frequency with three levels. To account for multiple comparisons, a cluster forming threshold of  $p < .001$  and cluster-extent threshold of  $k > 10$  (i.e., at least 640 mm<sup>3</sup> of brain tissue) were used, based on Gaussian random fields theory (Poline et al., 1995; Worsley et al., 1996). In addition, any

cluster falling within 4 cm of either seed voxel was excluded (Brookes et al., 2011).

## 3 | RESULTS

### 3.1 | Sensor-level neural responses

Sensor-level time-frequency analysis across all participants revealed significant oscillatory responses in a large number of posterior sensors for each base entrainment frequency (32 Hz, 40 Hz, and 48 Hz), as well as harmonics of the stimulation frequencies, all of which showed increased amplitude relative to baseline ( $p < .001$ , corrected; Figure 2). Given the goal of the study, we focused on 2 Hz wide bands centered on each entrainment frequency and the time window with the strongest response amplitude, which was 500–1000 ms following the onset of the flickering stimulus. We did not image the harmonics.

### 3.2 | Entrainment condition differences in oscillatory activity

As described in the methods (Section 2.6), entrainment responses were extracted from peak voxels identified in the grand averaged

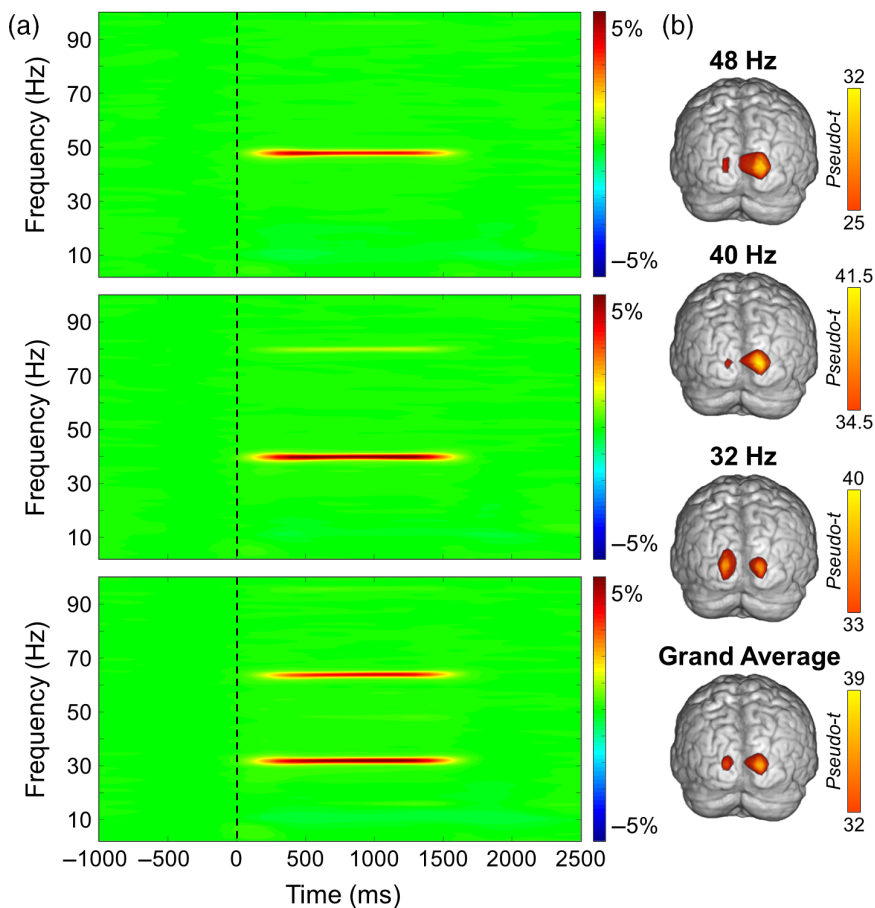


**FIGURE 2** Sensor and source level activity during visual entrainment. (a) Averaged time-frequency spectrograms from a posterior sensor (MEG2343) for 48 Hz (top), 40 Hz (middle), and 32 Hz (bottom) entrainment conditions. Time (ms) is shown on the x-axis and frequency (Hz) on the y-axis, and the color scale illustrates the percent change in oscillatory power relative to the baseline period (−600 to 0 ms). Clear entrainment can be seen at each fundamental driving frequency, and at the 2nd harmonic for the 40 and 32 Hz conditions. (b) Mean beamformer images (pseudo-t; see color bar) of the entrainment frequency for (from top to bottom) the 48, 40, and 32 Hz conditions, as well as the grand average of all three entrainment conditions. The functional images show that entrainment peaked in a consistent primary occipital cortical region for each stimulation frequency.



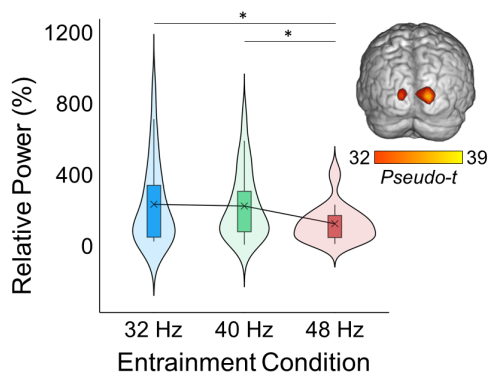


**FIGURE 3** Oscillatory power at each entrainment frequency. The brain map (top right) depicts the average entrainment response across all three entrainment conditions and all participants (i.e., the grand average). The box plots illustrate the entrainment response from 500 to 1000 ms for each frequency condition separately, which was extracted from bilateral occipital peaks depicted in the brain map and averaged across hemispheres. The X denotes the mean, the box edges are the first and third quartiles, and the whiskers indicate the minima and maxima. The surrounding violin plots illustrate the probability density. A repeated measures ANOVA revealed that the entrainment response was strongest for 32 and 40 Hz relative to 48 Hz ( $F_{2,48} = 5.98, p = .005$ ).

response maps (i.e., brain maps averaged across the three entrainment conditions and all participants). Statistical analysis of oscillatory power (i.e., changes in power relative to the baseline) revealed an overall effect of stimulation frequency ( $F_{2,48} = 5.98, p = .005$ ; Figure 3) and follow-up tests revealed that the 48 Hz entrainment response was weaker than the 32 ( $t_{24} = 2.81, p = .01$ ) and 40 Hz ( $t_{25} = 3.73, p < .001$ ) responses. No difference was observed between 32 and 40 Hz ( $t_{25} = -0.44, p = .97$ ).

### 3.3 | Habituation of oscillatory activity

The linear mixed effects (LME) model indicated that the entrainment response decreased across trials (i.e., habituated;  $b = -0.004, SD = .001, t_{1797} = -2.95$ ; Figure 4). Analysis of the simple slopes for each entrainment frequency separately revealed that this habituation effect was significant for the 32 Hz ( $b = -0.41, p = .003$ ) and 40 Hz ( $b = -0.36, p = .02$ ) entrainment response, but not the 48 Hz response ( $b = -0.15, p = .29$ ).

### 3.4 | Functional connectivity

We tested if functional connectivity at the entrainment frequency between the visual cortical seed regions and the brain differed across entrainment frequencies using a voxel-wise repeated-measures ANOVA. This analysis revealed two significant clusters, located in left inferior parietal lobule ( $F_{2,38} = 8.56, p < .001$ ) and left precentral gyrus (Figure 5;  $F_{2,38} = 9.18, p < .001$ ). Post hoc pair-wise comparisons

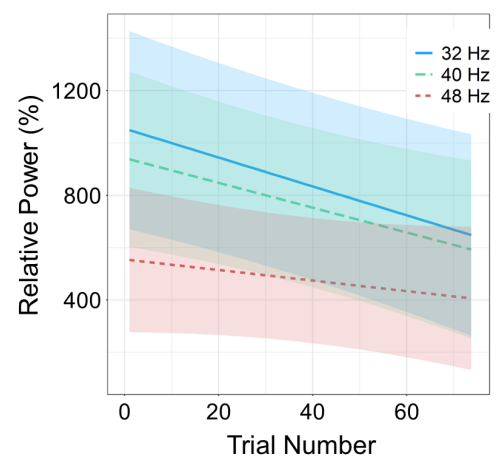


**FIGURE 4** Habituation of entrainment responses. The entrainment response amplitude (% change relative to baseline) per stimulation frequency is displayed on the y-axis, and trial number is on the x-axis. The lines represent the slope of the entrainment response decrease over trials (i.e., habituation) per condition, with the shading surrounding each line indicating the standard error of the mean. Linear mixed effects (LME) analyses revealed that the 32 ( $p < .001$ ) and 40 Hz ( $p = .02$ ) entrainment responses habituated, such that the responses became weaker as a function of trial number. However, this effect was not present at the 48 Hz stimulation frequency ( $p = .29$ ).

were conducted on the peak-voxel in each cluster. In the left precentral gyrus, connectivity was stronger for 40 relative to 32 ( $t_{19} = 3.85, p < .001$ ) and 48 Hz ( $t_{19} = 3.38, p = .003$ ) and did not differ between 32 and 48 Hz ( $t_{19} = 0.01, p = .99$ ). In the inferior parietal lobule, connectivity was weaker for 32 relative to 40 ( $t_{19} = -3.63, p = .002$ ) and 48 Hz ( $t_{19} = -3.43, p = .003$ ) and did not differ between 40 and 48 Hz ( $t_{19} = 0.97, p = .34$ ).

## 4 | DISCUSSION

In the current study, we tested which gamma-band frequency (32, 40, or 48 Hz) elicited the strongest entrainment response in visual cortex in a sample of healthy young adults. All three stimulation frequencies produced strong entrainment responses in primary visual cortex. We found that the entrainment response was strongest for 32 and 40 Hz relative to 48 Hz. In addition, entrainment at both 32 and 40 Hz, but not 48 Hz, showed a typical pattern of habituation across trials. These results suggest that, within the gamma frequency range, neural ensembles in visual cortex tend to synchronize more readily (i.e., resonate) at 32 and 40 Hz relative to 48 Hz. The implications of these findings on gamma entrainment therapy and the functional relevance of visual cortical gamma activity are discussed below.

Visual entrainment in the gamma band has recently received increased interest in part due to its potential therapeutic utility in AD, where repeated sessions of 40 Hz visual stimulation have been linked to reduced amyloid- $\beta$  and hyperphosphorylated tau in animals (Adaikkan et al., 2019; Hu et al., 2023; Iaccarino et al., 2016; Martorell

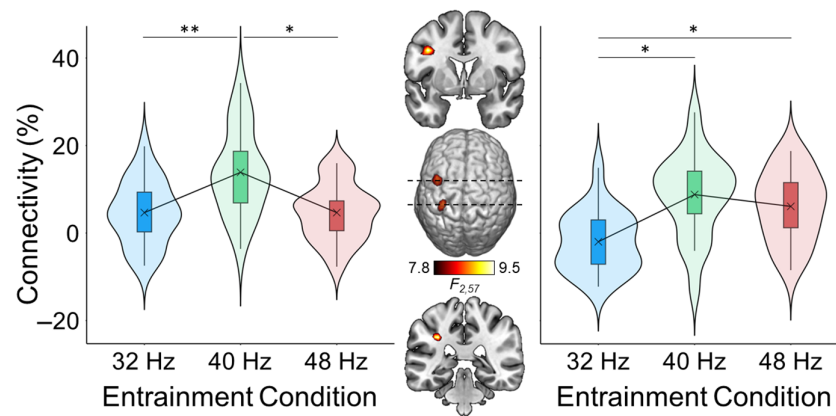


**FIGURE 5** Differences in functional connectivity between the visual cortex and the whole brain at each entrainment frequency. The brain map (middle) depicts the voxel-wise ANOVA, which compared the connectivity between each voxel and the primary visual cortex at the entrainment frequency for each entrainment condition. The box plots illustrate the strength of connectivity for the left precentral gyrus (left) and the left inferior parietal lobule (right) for each entrainment condition. The X denotes the mean, the box edges are the first and third quartiles, and the whiskers indicate the minima and maxima. The surrounding violin plots illustrate the probability density. \* $p < .01$ ; \*\* $p < .001$ .

et al., 2019). At least preliminary evidence points to similar findings in human trials, including a reduction in the clinical manifestations of AD (Chan et al., 2022; Cimenser et al., 2021; Clements-Cortes et al., 2016; He et al., 2021; Hu et al., 2023; Manippa et al., 2022; Traikapi & Konstantinou, 2021), but not a reduction in amyloid- $\beta$  (He et al., 2021; Ismail et al., 2018). While limited, the available evidence suggests that the therapeutic effects are related to the degree of local entrainment and are confined to neural tissue that entrains the flickering stimulus to a moderately high level (Iaccarino et al., 2016). Thus, identifying the stimulation parameters that lead to the greatest amplitude and volume of neural tissue being entrained would be advantageous to such therapeutic approaches, and may lead to better outcomes in humans. Our current findings suggest that 32 and 40 Hz compared to 48 Hz elicited the strongest entrainment response, indicative of the synchronization of more local neural cells entraining to the stimulus (Pfurtscheller et al., 1996). While AD therapies have focused on 40 Hz photic stimulation, these results suggest that gamma frequencies below 40 Hz may be equally as effective insofar as they excite the same proportion of neural tissue, but ineffective at higher gamma frequencies.

While numerous studies have established that the strongest visual entrainment response typically occurs with 14–16 Hz stimulation (Herrmann, 2001; Lazarev et al., 2001; Pastor et al., 2003, 2007), few studies have examined entrainment responses within the gamma range. The classic experiment by Herrmann et al. (2001), where the entrainment response was tested across frequencies ranging from 1 to 100 Hz, reported a stronger entrainment response at 40 Hz compared to the neighboring frequencies. In contrast, a recent study (Gulbinaite et al., 2019) found strongest responses in the gamma range at  $\sim 47$  Hz compared to lower frequencies in the gamma range (including 32 and 40 Hz). However, the results from Gulbinaite et al. (2019) also disagree with Pastor et al. (2003), who found weaker entrainment responses at 47 Hz compared to neighboring frequencies. In fact, Pastor et al. (2003) reported the strongest gamma band

responses at 30 and 35 Hz compared to higher gamma frequencies, consistent with our current findings. Similarly, both Park et al. (2022) and Lee et al. (2021) found stronger entrainment at around 30 to 35 Hz compared to higher gamma frequencies. Taken together, our results agree with the majority of the limited extant literature and provide evidence favoring visual stimulation at 32 and 40 Hz.

We also examined connectivity differences at the entrainment frequencies between each voxel in the brain and the peak entrainment voxel within visual cortex. Overall, stronger connectivity was observed predominantly at 40 Hz in prefrontal and parietal cortices; connectivity in the parietal region did not differ between 40 and 48 Hz. The current results partially disagree with recent EEG studies where connectivity was stronger at entrainment frequencies  $< 40$  Hz (Lee et al., 2021; Park et al., 2022). The discrepant results in these studies may be due to our calculation being in source space, whereas connectivity in these other studies was conducted at the electrode level between posterior and anterior electrodes. These results suggest that visual information may propagate between primary visual and higher tier attention cortices more efficiently at 40 Hz compared to lower and higher gamma-band frequencies. This is particularly relevant to AD therapies, where more widespread entrainment across the brain could increase the potential to alleviate AD biomarkers. Notably, the precuneus/inferior parietal cortices has particularly high AB deposition in the earlier stages of AD (Palmqvist et al., 2017). Thus, visual entrainment at 40 Hz may be best suited to invoke the therapeutic effects of gamma-band treatment in relevant brain regions.

Beyond therapeutic relevance, gamma-band entrainment is pertinent to the study of visual cortical function in general. Visual gamma activity is thought to be essential to information processing within local neural circuits (Tallon-Baudry, 2009; Uhlhaas et al., 2009), including the binding of low-level visual features in perception (Fries et al., 2001; Keil et al., 1999; Tallon-Baudry & Bertrand, 1999), and is strongly tied to GABAergic signaling (Balz et al., 2016; Buzsáki & Wang, 2012; Chen et al., 2014; Edden et al., 2009; Gaetz et al., 2011;



Kujala et al., 2015; Muthukumaraswamy et al., 2009). The stronger entrainment responses at 32 and 40 Hz relative to 48 Hz suggests that neural ensembles, which endogenously operate within the gamma-band and involve GABAergic signaling, tend to resonate at these lower gamma-band frequencies rather than higher frequencies. However, further work is needed. Future studies should consider a broader array of gamma entrainment parameters to pinpoint the optimal approach and should also test of individual differences in preferred gamma flicker frequency.

The entrainment response to both 32 and 40 Hz, but not 48 Hz, habituated across trials. Evoked responses in sensory cortex to nonarousing stimuli have long been shown to habituate with repetition (Abdulhussein et al., 2022; Megela & Teyler, 1979; Rauschel et al., 2016; Schupp et al., 2006). While the precise mechanism of habituation is not fully characterized, the habituation of sensory responses to redundant stimulation has been widely documented (Megela & Teyler, 1979; Schoenen, 1996; Thompson & Spencer, 1966). Interestingly, cortical responses show no habituation in disorders involving sensory processing (e.g., migraine with aura, autism; (Dwyer et al., 2023; Harriott & Schwedt, 2014; Rauschel et al., 2016)), which work (albeit limited) has suggested is due to aberrant GABAergic signaling from interneurons (Palermo et al., 2011). Given the relevance of GABA to both AD therapy and visual cortical gamma function more generally, as discussed above, habituation patterns of entrained stimuli may be of interest for future entrainment therapy work.

Other work has used brain stimulation at 40 Hz as a therapeutic approach to AD and mild cognitive impairment (MCI). While the precise location of stimulation has differed across studies (Manippa, Palmisano, et al., 2024), converging evidence indicates that 40 Hz tACS improves cognitive and memory skills (Benussi et al., 2021, 2022; Kehler et al., 2020; Kim et al., 2021; Moussavi et al., 2021; Naro et al., 2016; Zhou et al., 2022; but see Sprugnoli et al., 2021), and limited evidence has shown changes in some AD biomarkers (Dhaynaut et al., 2022; Zhou et al., 2022). Drawing from animal work, researchers have proposed that the improvements in cognition following tACS therapy results from increases in the activity of inhibitory interneurons (Manippa, Palmisano, et al., 2024), which are dysfunctional (Palop & Mucke, 2016; Styr & Slutsky, 2018) and the root of large-scale excitatory-inhibitory imbalance in AD (Hijazi et al., 2020). In addition, some speculate that gamma-band excitation may directly induce a microglia response to reduce amyloid- $\beta$  and p-tau burden (Adaikkan & Tsai, 2020). Future work may consider the effect of entrainment frequency on these neurobiological processes, rather than strictly on strength of entrainment per se.

Before closing, several limitations should be noted. First, a limited number of frequencies were investigated in order to keep the MEG recording as short as possible while also obtaining sufficient numbers of trials for beamformer source reconstruction, and we focused on those surrounding 40 Hz given the recent work surrounding emerging AD therapies. Future work should investigate higher segments of the gamma band, the 70–90 Hz range where robust motor responses are often found (Fung et al., 2022; Meehan et al., 2023; Spooner

et al., 2021; Trevarrow et al., 2019; Wiesman, Christopher-Hayes, et al., 2021). Second, entrainment was driven by only one type of stimulus (a white dot). The visual entrainment response is indeed sensitive to the spatial characteristics (Nguyen et al., 2017; Vialatte et al., 2010) or color (Lee et al., 2021) of the flickering stimulus and different stimulus types have been localized to different regions in the visual hierarchy (Gundlach & Müller, 2013; Regan, 1989; Rossion, 2014). Future studies could explore the impact of stimulus characteristics on entrainment in the gamma band, with the premise that higher order visual regions may be more susceptible to entrainment if the stimulus was more complex. Along these lines, diffuse light sources have been shown to differentially effect brain activity (Kasteleijn-Nolst Trenité et al., 2012; Leijten et al., 1998), and may be relevant to the efficacy of gamma-band entrainment therapies.

To summarize, we found stronger visual entrainment responses at 32 and 40 Hz compared to 48 Hz, suggesting that neural ensemble activity within the gamma band tends to resonate, and thus entrain more readily, when stimulated at these relatively low gamma range frequencies. Entrainment therapies for AD have focused on 40 Hz, but these results suggest that lower frequencies may be equally suited for such approaches; at the same time, frequencies above 40 Hz appear to be less ideal. Adding to this notion, 32 and 40 Hz stimulation were associated with habituation across the duration of the experiment, but the same was not found for 48 Hz. Finally, whole-brain connectivity patterns with visual cortex tended to be strongest at 40 Hz. Beyond therapeutic relevance, these results constitute ideal parameters to study visual gamma band activity in general, which has been strongly tied to GABAergic signaling (Balz et al., 2016; Chen et al., 2014; Edden et al., 2009; Gaetz et al., 2011; Muthukumaraswamy et al., 2009).

## ACKNOWLEDGMENTS

This study was supported by the National Institutes of Health through grants R01-MH116782 (TWW), R01-MH118013 (TWW), S10-OD028751 (TWW), R01-DA047828 (TWW), R01-DA056223 (TWW), P20-GM144641 (TWW), and F30-AG076259 (SDS). The funders had no role in the study design, collection, analysis, or interpretation of data, nor did they influence writing the report or the decision to submit this work for publication.

## CONFLICT OF INTEREST STATEMENT

All authors report no biomedical financial interests or potential conflicts of interest.

## DATA AVAILABILITY STATEMENT

The data used in this article will be made publicly available through the COINS framework at the completion of the study (<https://coins.trendscenter.org/>).

## PATIENT CONSENT STATEMENT

The Institutional Review Board reviewed and approved this investigation. Each participant provided written informed consent following a detailed description of the study.

## ORCID

Nathan M. Petro  <https://orcid.org/0000-0002-7553-4459>

Lauren K. Weibert  <https://orcid.org/0009-0001-3075-479X>

Tony W. Wilson  <https://orcid.org/0000-0002-5053-8306>

## REFERENCES

- Abdulhussein, M. A., An, X., Alsakaa, A. A., & Ming, D. (2022). Lack of habituation in migraine patients and evoked potential types: Analysis study from EEG signals. *Journal of Information and Optimization Sciences*, 43(4), 855–891. <https://doi.org/10.1080/02522667.2022.2095958>
- Adaikkan, C., Middleton, S. J., Marco, A., Pao, P.-C., Mathys, H., Kim, D. N.-W., Gao, F., Young, J. Z., Suk, H.-J., Boyden, E. S., McHugh, T. J., & Tsai, L.-H. (2019). Gamma entrainment binds higher-order brain regions and offers neuroprotection. *Neuron*, 102(5), 929–943.e8. <https://doi.org/10.1016/j.neuron.2019.04.011>
- Adaikkan, C., & Tsai, L.-H. (2020). Gamma entrainment: Impact on neuro-circuits, glia, and therapeutic opportunities. *Trends in Neurosciences*, 43(1), 24–41. <https://doi.org/10.1016/j.tins.2019.11.001>
- Angelini, L., de Tommaso, M., Guido, M., Hu, K., Ivanov, P. C., Marinazzo, D., Nardulli, G., Nitti, L., Pellicoro, M., Pierro, C., & Stramaglia, S. (2004). Steady-state visual evoked potentials and phase synchronization in migraine patients. *Physical Review Letters*, 93(3), 038103. <https://doi.org/10.1103/PhysRevLett.93.038103>
- Arif, Y., Wiesman, A. I., O'Neill, J., Embury, C., May, P. E., Lew, B. J., Schantell, M. D., Fox, H. S., Swindells, S., & Wilson, T. W. (2020). The age-related trajectory of visual attention neural function is altered in adults living with HIV: A cross-sectional MEG study. *eBioMedicine*, 61, 103065. <https://doi.org/10.1016/j.ebiom.2020.103065>
- Balz, J., Keil, J., Roa Romero, Y., Mекle, R., Schubert, F., Aydin, S., Ittermann, B., Gallinat, J., & Senkowski, D. (2016). GABA concentration in superior temporal sulcus predicts gamma power and perception in the sound-induced flash illusion. *NeuroImage*, 125, 724–730. <https://doi.org/10.1016/j.neuroimage.2015.10.087>
- Benussi, A., Cantoni, V., Cotelli, M. S., Cotelli, M., Brattini, C., Datta, A., Thomas, C., Santarnecchi, E., Pascual-Leone, A., & Borroni, B. (2021). Exposure to gamma tACS in Alzheimer's disease: A randomized, double-blind, sham-controlled, crossover, pilot study. *Brain Stimulation*, 14(3), 531–540. <https://doi.org/10.1016/j.brs.2021.03.007>
- Benussi, A., Cantoni, V., Grassi, M., Brechet, L., Michel, C. M., Datta, A., Thomas, C., Gazzina, S., Cotelli, M. S., Bianchi, M., Premi, E., Gadola, Y., Cotelli, M., Pengo, M., Perrone, F., Sclaro, M., Archetti, S., Solje, E., Padovani, A., ... Borroni, B. (2022). Increasing brain gamma activity improves episodic memory and restores cholinergic dysfunction in Alzheimer's disease. *Annals of Neurology*, 92(2), 322–334. <https://doi.org/10.1002/ana.26411>
- Bi, D., Wen, L., Wu, Z., & Shen, Y. (2020). GABAergic dysfunction in excitatory and inhibitory (E/I) imbalance drives the pathogenesis of Alzheimer's disease. *Alzheimer's & Dementia: The Journal of the Alzheimer's Association*, 16(9), 1312–1329. <https://doi.org/10.1002/alz.12088>
- Brookes, M. J., Hale, J. R., Zumer, J. M., Stevenson, C. M., Francis, S. T., Barnes, G. R., Owen, J. P., Morris, P. G., & Nagarajan, S. S. (2011). Measuring functional connectivity using MEG: Methodology and comparison with fMRI. *NeuroImage*, 56(3), 1082–1104. <https://doi.org/10.1016/j.neuroimage.2011.02.054>
- Buzsáki, G., & Wang, X.-J. (2012). Mechanisms of gamma oscillations. *Annual Review of Neuroscience*, 35(1), 203–225. <https://doi.org/10.1146/annurev-neuro-062111-150444>
- Casagrande, C. C., Lew, B. J., Taylor, B. K., Schantell, M., O'Neill, J., May, P. E., Swindells, S., & Wilson, T. W. (2021). Impact of HIV-infection on human somatosensory processing, spontaneous cortical activity, and cortical thickness: A multimodal neuroimaging approach. *Human Brain Mapping*, 42(9), 2851–2861. <https://doi.org/10.1002/hbm.25408>
- Casagrande, C. C., Wiesman, A. I., Schantell, M., Johnson, H. J., Wolfson, S. L., O'Neill, J., Johnson, C. M., May, P. E., Swindells, S., Murman, D. L., & Wilson, T. W. (2022). Signatures of somatosensory cortical dysfunction in Alzheimer's disease and HIV-associated neuro-cognitive disorder. *Brain Communications*, 4(4), fcac169. <https://doi.org/10.1093/braincomms/fcac169>
- Chan, D., Suk, H.-J., Jackson, B. L., Milman, N. P., Stark, D., Klerman, E. B., Kitchener, E., Avalos, V. S. F., Weck, G. d., Banerjee, A., Beach, S. D., Blanchard, J., Stearns, C., Boes, A. D., Uitermarkt, B., Gander, P., Iii, M. H., Sternberg, E. J., Nieto-Castanon, A., ... Tsai, L.-H. (2022). Gamma frequency sensory stimulation in mild probable Alzheimer's dementia patients: Results of feasibility and pilot studies. *PLoS One*, 17(12), e0278412. <https://doi.org/10.1371/journal.pone.0278412>
- Chen, C.-M. A., Stanford, A. D., Mao, X., Abi-Dargham, A., Shungu, D. C., Lisanby, S. H., Schroeder, C. E., & Kegeles, L. S. (2014). GABA level, gamma oscillation, and working memory performance in schizophrenia. *NeuroImage: Clinical*, 4, 531–539. <https://doi.org/10.1016/j.nicl.2014.03.007>
- Cimenser, A., Hempel, E., Travers, T., Strozewski, N., Martin, K., Malchano, Z., & Hajós, M. (2021). Sensory-evoked 40-Hz gamma oscillation improves sleep and daily living activities in Alzheimer's disease patients. *Frontiers in Systems Neuroscience*, 15, 746859. <https://doi.org/10.3389/fnsys.2021.746859>
- Clements-Cortes, A., Ahonen, H., Evans, M., Freedman, M., & Bartel, L. (2016). Short-term effects of rhythmic sensory stimulation in Alzheimer's disease: An exploratory pilot study. *Journal of Alzheimer's Disease*, 52(2), 651–660. <https://doi.org/10.3233/JAD-160081>
- Clementz, B. A., Keil, A., & Kissler, J. (2004). Aberrant brain dynamics in schizophrenia: Delayed buildup and prolonged decay of the visual steady-state response. *Brain Research. Cognitive Brain Research*, 18(2), 121–129. <https://doi.org/10.1016/j.cogbrainres.2003.09.007>
- Dalal, S. S., Sekihara, K., & Nagarajan, S. S. (2006). Modified beamformers for coherent source region suppression. *IEEE Transactions on Bio-Medical Engineering*, 53(7), 1357–1363. <https://doi.org/10.1109/TBME.2006.873752>
- Dhaynaut, M., Sprugnoli, G., Cappon, D., Macone, J., Sanchez, J. S., Normandin, M. D., Guehl, N. J., Koch, G., Paciorek, R., Connor, A., Press, D., Johnson, K., Pascual-Leone, A., El Fakhri, G., & Santarnecchi, E. (2022). Impact of 40 Hz transcranial alternating current stimulation on cerebral tau burden in patients with Alzheimer's disease: A case series. *Journal of Alzheimer's Disease*, 85(4), 1667–1676. <https://doi.org/10.3233/JAD-215072>
- Di Russo, F., Pitzalis, S., Aprile, T., Spitoni, G., Patria, F., Stella, A., Spinelli, D., & Hillyard, S. A. (2007). Spatiotemporal analysis of the cortical sources of the steady-state visual evoked potential. *Human Brain Mapping*, 28(4), 323–334. <https://doi.org/10.1002/hbm.20276>
- Dwyer, P., Williams, Z. J., Vukusic, S., Saron, C. D., & Rivera, S. M. (2023). Habituation of auditory responses in young autistic and neurotypical children. *Autism Research*, aur.3022, 1903–1923. <https://doi.org/10.1002/aur.3022>
- Edden, R. A. E., Muthukumaraswamy, S. D., Freeman, T. C. A., & Singh, K. D. (2009). Orientation discrimination performance is predicted by GABA concentration and gamma oscillation frequency in human primary visual cortex. *Journal of Neuroscience*, 29(50), 15721–15726. <https://doi.org/10.1523/JNEUROSCI.4426-09.2009>
- Enomoto, T., Tse, M. T., & Floresco, S. B. (2011). Reducing prefrontal gamma-aminobutyric acid activity induces cognitive, behavioral, and dopaminergic abnormalities that resemble schizophrenia. *Biological Psychiatry*, 69(5), 432–441. <https://doi.org/10.1016/j.biopsych.2010.09.038>
- Ernst, M. D. (2004). Permutation methods: A basis for exact inference. *Statistical Science*, 19(4), 676–685. <https://doi.org/10.1214/088342304000000396>

- Fries, P., Reynolds, J. H., Rorie, A. E., & Desimone, R. (2001). Modulation of oscillatory neuronal synchronization by selective visual attention. *Science*, (New York, N.Y.), 291(5508), 1560–1563. <https://doi.org/10.1126/science.1055465>
- Fung, M. H., Heinrichs-Graham, E., Taylor, B. K., Frenzel, M. R., Eastman, J. A., Wang, Y.-P., Calhoun, V. D., Stephen, J. M., & Wilson, T. W. (2022). The development of sensorimotor cortical oscillations is mediated by pubertal testosterone. *NeuroImage*, 264, 119745. <https://doi.org/10.1016/j.neuroimage.2022.119745>
- Gaetz, W., Edgar, J. C., & Roberts, D. J. W. T. P. L. (2011). Relating MEG measured motor cortical oscillations to resting  $\gamma$ -aminobutyric acid (GABA) concentration. *NeuroImage*, 55(2), 616–621. <https://doi.org/10.1016/j.neuroimage.2010.12.077>
- Groff, B. R., Wiesman, A. I., Rezych, M. T., O'Neill, J., Robertson, K. R., Fox, H. S., Swindells, S., & Wilson, T. W. (2020). Age-related visual dynamics in HIV-infected adults with cognitive impairment. *Neurology® Neuroimmunology & Neuroinflammation*, 7(3), e690. <https://doi.org/10.1212/NXI.0000000000000690>
- Gross, J., Kujala, J., Hämäläinen, M., Timmermann, L., Schnitzler, A., & Salmelin, R. (2001). Dynamic imaging of coherent sources: Studying neural interactions in the human brain. *Proceedings of the National Academy of Sciences*, 98(2), 694–699. <https://doi.org/10.1073/pnas.98.2.694>
- Gulbinaite, R., Roozendaal, D. H. M., & VanRullen, R. (2019). Attention differentially modulates the amplitude of resonance frequencies in the visual cortex. *NeuroImage*, 203, 116146. <https://doi.org/10.1016/j.neuroimage.2019.116146>
- Gundlach, C., & Müller, M. M. (2013). Perception of illusory contours forms intermodulation responses of steady state visual evoked potentials as a neural signature of spatial integration. *Biological Psychology*, 94(1), 55–60. <https://doi.org/10.1016/j.biopsycho.2013.04.014>
- Güntekin, B., Emek-Savaş, D. D., Kurt, P., Yener, G. G., & Başar, E. (2013). Beta oscillatory responses in healthy subjects and subjects with mild cognitive impairment. *NeuroImage: Clinical*, 3, 39–46. <https://doi.org/10.1016/j.nicl.2013.07.003>
- Harriott, A. M., & Schwedt, T. J. (2014). Migraine is associated with altered processing of sensory stimuli. *Current Pain and Headache Reports*, 18(11), 458. <https://doi.org/10.1007/s11916-014-0458-8>
- He, Q., Colon-Motas, K. M., Pybus, A. F., Piendel, L., Seppa, J. K., Walker, M. L., Manzanares, C. M., Qiu, D., Miocinovic, S., Wood, L. B., Levey, A. I., Lah, J. J., & Singer, A. C. (2021). A feasibility trial of gamma sensory flicker for patients with prodromal Alzheimer's disease. *Alzheimer's & Dementia: Translational Research & Clinical Interventions*, 7(1), e12178. <https://doi.org/10.1002/trc2.12178>
- Heinrichs-Graham, E., McDermott, T. J., Mills, M. S., Coolidge, N. M., & Wilson, T. W. (2017). Transcranial direct-current stimulation modulates offline visual oscillatory activity: A magnetoencephalography study. *Cortex*, 88, 19–31. <https://doi.org/10.1016/j.cortex.2016.11.016>
- Herrmann, C. S. (2001). Human EEG responses to 1–100 Hz flicker: Resonance phenomena in visual cortex and their potential correlation to cognitive phenomena. *Experimental Brain Research*, 137(3), 346–353. <https://doi.org/10.1007/s002210100682>
- Hijazi, S., Heistek, T. S., Scheltens, P., Neumann, U., Shimshek, D. R., Mansvelder, H. D., Smit, A. B., & van Kesteren, R. E. (2020). Early restoration of parvalbumin interneuron activity prevents memory loss and network hyperexcitability in a mouse model of Alzheimer's disease. *Molecular Psychiatry*, 25(12), 3380–3398. <https://doi.org/10.1038/s41380-019-0483-4>
- Hillebrand, A., Singh, K. D., Holliday, I. E., Furlong, P. L., & Barnes, G. R. (2005). A new approach to neuroimaging with magnetoencephalography. *Human Brain Mapping*, 25(2), 199–211. <https://doi.org/10.1002/hbm.20102>
- Hillyard, S. A., Hinrichs, H., Tempelmann, C., Morgan, S. T., Hansen, J. C., Scheich, H., & Heinze, H.-J. (1997). Combining steady-state visual evoked potentials and fMRI to localize brain activity during selective attention. *Human Brain Mapping*, 5(4), 287–292. [https://doi.org/10.1002/\(SICI\)1097-0193\(1997\)5:4<287::AID-HBM14>3.0.CO;2-B](https://doi.org/10.1002/(SICI)1097-0193(1997)5:4<287::AID-HBM14>3.0.CO;2-B)
- Hoehstetter, K., Bornfleth, H., Weckesser, D., Ille, N., Berg, P., & Scherg, M. (2004). BESA source coherence: A new method to study cortical oscillatory coupling. *Brain Topography*, 16(4), 233–238. <https://doi.org/10.1023/b:brat.0000032857.55223.5d>
- Hu, J., Zheng, L., Guan, Z., Zhong, K., Huang, F., Huang, Q., Yang, J., Li, W., & Li, S. (2023). Sensory gamma entrainment: Impact on amyloid protein and therapeutic mechanism. *Brain Research Bulletin*, 202, 110750. <https://doi.org/10.1016/j.brainresbull.2023.110750>
- Iaccarino, H. F., Singer, A. C., Martorell, A. J., Rudenko, A., Gao, F., Gillingham, T. Z., Mathys, H., Seo, J., Kritskiy, O., Abdurrob, F., Adaikkan, C., Canter, R. G., Rueda, R., Brown, E. N., Boyden, E. S., & Tsai, L.-H. (2016). Gamma frequency entrainment attenuates amyloid load and modifies microglia. *Nature*, 540(7632), 230–235. <https://doi.org/10.1038/nature20587>
- Ismail, R., Hansen, A. K., Parbo, P., Brændgaard, H., Gottrup, H., Brooks, D. J., & Borghammer, P. (2018). The effect of 40-Hz light therapy on amyloid load in patients with prodromal and clinical Alzheimer's disease. *International Journal of Alzheimer's Disease*, 2018, e6852303. <https://doi.org/10.1155/2018/6852303>
- Jafari, Z., Kolb, B. E., & Mohajeri, M. H. (2020). Neural oscillations and brain stimulation in Alzheimer's disease. *Progress in Neurobiology*, 194, 101878. <https://doi.org/10.1016/j.pneurobio.2020.101878>
- Jensen, O., Kaiser, J., & Lachaux, J.-P. (2007). Human gamma-frequency oscillations associated with attention and memory. *Trends in Neurosciences*, 30(7), 317–324. <https://doi.org/10.1016/j.tins.2007.05.001>
- Jiménez-Balado, J., & Eich, T. S. (2021). GABAergic dysfunction, neural network hyperactivity and memory impairments in human aging and Alzheimer's disease. *Seminars in Cell & Developmental Biology*, 116, 146–159. <https://doi.org/10.1016/j.semdb.2021.01.005>
- Jin, Y., Castellanos, A., Solis, E. R., & Potkin, S. G. (2000). EEG resonant responses in schizophrenia: A photic driving study with improved harmonic resolution. *Schizophrenia Research*, 44(3), 213–220. [https://doi.org/10.1016/S0920-9964\(99\)00211-X](https://doi.org/10.1016/S0920-9964(99)00211-X)
- Kasteleijn-Nolst Trenité, D., Rubboli, G., Hirsch, E., Martins da Silva, A., Seri, S., Wilkins, A., Parra, J., Covanis, A., Elia, M., Capovilla, G., Stephani, U., & Harding, G. (2012). Methodology of photic stimulation revisited: Updated European algorithm for visual stimulation in the EEG laboratory. *Epilepsia*, 53(1), 16–24. <https://doi.org/10.1111/j.1528-1167.2011.03319.x>
- Kehler, L., Francisco, C. O., Uehara, M. A., & Moussavi, Z. (2020). The effect of transcranial alternating current stimulation (tACS) on cognitive function in older adults with dementia. *Annual International Conference of the IEEE Engineering in Medicine and Biology Society. IEEE Engineering in Medicine and Biology Society. Annual International Conference*, 2020, 3649–3653. <https://doi.org/10.1109/EMBC44109.2020.9175903>
- Keil, A., Müller, M. M., Ray, W. J., Gruber, T., & Elbert, T. (1999). Human gamma band activity and perception of a gestalt. *Journal of Neuroscience*, 19(16), 7152–7161. <https://doi.org/10.1523/JNEUROSCI.19-16-07152.1999>
- Kim, J., Kim, H., Jeong, H., Roh, D., & Kim, D. H. (2021). tACS as a promising therapeutic option for improving cognitive function in mild cognitive impairment: A direct comparison between tACS and tDCS. *Journal of Psychiatric Research*, 141, 248–256. <https://doi.org/10.1016/j.jpsyires.2021.07.012>
- Kleiner, M., Brainard, D., Pelli, D., Ingling, A., Murray, R., & Broussard, C. (2007). What's new in psychtoolbox-3. *Perception*, 36(14), 1–16.
- Kocagoncu, E., Quinn, A., Firouzian, A., Cooper, E., Greve, A., Gunn, R., Green, G., Woolrich, M. W., Henson, R. N., Lovestone, S., & Rowe, J. B. (2020). Tau pathology in early Alzheimer's disease is linked to selective disruptions in neurophysiological network dynamics. *Neurobiology of Aging*, 92, 141–152. <https://doi.org/10.1016/j.neurobiolaging.2020.03.009>

- Koch, G., Casula, E. P., Bonni, S., Borghi, I., Assogna, M., Minei, M., Pellicciari, M. C., Motta, C., D'Acunto, A., Porrazzini, F., Maiella, M., Ferrari, C., Caltagirone, C., Santarnecchi, E., Bozzali, M., & Martorana, A. (2022). Precuneus magnetic stimulation for Alzheimer's disease: A randomized, sham-controlled trial. *Brain*, 145(11), 3776–3786. <https://doi.org/10.1093/brain/awac285>
- Kovach, C. K., & Gander, P. E. (2016). The demodulated band transform. *Journal of Neuroscience Methods*, 261, 135–154. <https://doi.org/10.1016/j.jneumeth.2015.12.004>
- Kujala, J., Jung, J., Bouvard, S., Lecaigard, F., Lothe, A., Bouet, R., Ciumas, C., Ryvlin, P., & Jerbi, K. (2015). Gamma oscillations in V1 are correlated with GABAA receptor density: A multi-modal MEG and Flumazenil-PET study. *Scientific Reports*, 5(1), 16347. <https://doi.org/10.1038/srep16347>
- Lazarev, V. V., Simpson, D. M., Schubsky, B. M., & deAzevedo, L. C. (2001). Photic driving in the electroencephalogram of children and adolescents: Harmonic structure and relation to the resting state. *Brazilian Journal of Medical and Biological Research*, 34, 1573–1584. <https://doi.org/10.1590/S0100-879X2001001200010>
- Lee, K., Park, Y., Suh, S. W., Kim, S.-S., Kim, D.-W., Lee, J., Park, J., Yoo, S., & Kim, K. W. (2021). Optimal flickering light stimulation for entraining gamma waves in the human brain. *Scientific Reports*, 11(1), 16206. <https://doi.org/10.1038/s41598-021-95550-1>
- Leijten, F. S., Dekker, E., Spekrijse, H., Kasteleijn-Nolst Trenité, D. G., & Van Emde Boas, W. (1998). Light diffusion in photosensitive epilepsy. *Electroencephalography and Clinical Neurophysiology*, 106(5), 387–391. [https://doi.org/10.1016/s0013-4694\(97\)00146-6](https://doi.org/10.1016/s0013-4694(97)00146-6)
- Lopes da Silva, F. (1991). Neural mechanisms underlying brain waves: From neural membranes to networks. *Electroencephalography and Clinical Neurophysiology*, 79(2), 81–93. [https://doi.org/10.1016/0013-4694\(91\)90044-5](https://doi.org/10.1016/0013-4694(91)90044-5)
- Manippa, V., Filardi, M., Vilella, D., Logroscino, G., & Rivolta, D. (2024). Gamma (60 Hz) auditory stimulation improves intrusions but not recall and working memory in healthy adults. *Behavioural Brain Research*, 456, 114703. <https://doi.org/10.1016/j.bbr.2023.114703>
- Manippa, V., Palmisano, A., Filardi, M., Vilella, D., Nitsche, M. A., Rivolta, D., & Logroscino, G. (2022). An update on the use of gamma (multi)sensory stimulation for Alzheimer's disease treatment. *Frontiers in Aging Neuroscience*, 14, 1095081. <https://doi.org/10.3389/fnagi.2022.1095081>
- Manippa, V., Palmisano, A., Nitsche, M. A., Filardi, M., Vilella, D., Logroscino, G., & Rivolta, D. (2024). Cognitive and neuropathophysiological outcomes of gamma-tACS in dementia: A systematic review. *Neuropsychology Review*, 34(1), 338–361. <https://doi.org/10.1007/s11065-023-09589-0>
- Maris, E., & Oostenveld, R. (2007). Nonparametric statistical testing of EEG- and MEG-data. *Journal of Neuroscience Methods*, 164(1), 177–190. <https://doi.org/10.1016/j.jneumeth.2007.03.024>
- Martorell, A. J., Paulson, A. L., Suk, H.-J., Abdurrob, F., Drummond, G. T., Guan, W., Young, J. Z., Kim, D. N.-W., Kritskiy, O., Barker, S. J., Mangena, V., Prince, S. M., Brown, E. N., Chung, K., Boyden, E. S., Singer, A. C., & Tsai, L.-H. (2019). Multi-sensory gamma stimulation ameliorates Alzheimer's-associated pathology and improves cognition. *Cell*, 177(2), 256–271.e22. <https://doi.org/10.1016/j.cell.2019.02.014>
- Meehan, C. E., Schantell, M., Springer, S. D., Wiesman, A. I., Wolfson, S. L., O'Neill, J., Murman, D. L., Bares, S. H., May, P. E., Johnson, C. M., & Wilson, T. W. (2023). Movement-related beta and gamma oscillations indicate parallels and disparities between Alzheimer's disease and HIV-associated neurocognitive disorder. *Neurobiology of Disease*, 186, 106283. <https://doi.org/10.1016/j.nbd.2023.106283>
- Megela, A. L., & Teyler, T. J. (1979). Habituation and the human evoked potential. *Journal of Comparative and Physiological Psychology*, 93(6), 1154–1170. <https://doi.org/10.1037/h0077630>
- Moussavi, Z., Kimura, K., Kehler, L., de Oliveira Francisco, C., & Lithgow, B. (2021). A novel program to improve cognitive function in individuals with dementia using transcranial alternating current stimulation (tACS) and tutored cognitive exercises. *Frontiers in Aging*, 2, 632545. <https://doi.org/10.3389/fragi.2021.632545>
- Muthukumaraswamy, S. D., Edden, R. A. E., Jones, D. K., Swettenham, J. B., & Singh, K. D. (2009). Resting GABA concentration predicts peak gamma frequency and fMRI amplitude in response to visual stimulation in humans. *Proceedings of the National Academy of Sciences*, 106(20), 8356–8361. <https://doi.org/10.1073/pnas.0900728106>
- Naro, A., Corallo, F., De Salvo, S., Marra, A., Di Lorenzo, G., Muscarà, N., Russo, M., Marino, S., De Luca, R., Bramanti, P., & Calabrò, R. S. (2016). Promising role of neuromodulation in predicting the progression of mild cognitive impairment to dementia. *Journal of Alzheimer's Disease*, 53(4), 1375–1388. <https://doi.org/10.3233/JAD-160305>
- Nguyen, T., Kuntzelman, K., & Miskovic, V. (2017). Entrainment of visual steady-state responses is modulated by global spatial statistics. *Journal of Neurophysiology*, 118(1), 344–352. <https://doi.org/10.1152/jn.00129.2017>
- Notbohm, A., Kurths, J., & Herrmann, C. S. (2016). Modification of brain oscillations via rhythmic light stimulation provides evidence for entrainment but not for superposition of event-related responses. *Frontiers in Human Neuroscience*, 10, 10. <https://doi.org/10.3389/fnhum.2016.00010>
- Palermo, A., Giglia, G., Vigneri, S., Cosentino, G., Fierro, B., & Brighina, F. (2011). Does habituation depend on cortical inhibition? Results of a rTMS study in healthy subjects. *Experimental Brain Research*, 212(1), 101–107. <https://doi.org/10.1007/s00221-011-2701-4>
- Palmqvist, S., Schöll, M., Strandberg, O., Mattsson, N., Stomrud, E., Zetterberg, H., Blennow, K., Landau, S., Jagust, W., & Hansson, O. (2017). Earliest accumulation of  $\beta$ -amyloid occurs within the default-mode network and concurrently affects brain connectivity. *Nature Communications*, 8(1), 1214. <https://doi.org/10.1038/s41467-017-01150-x>
- Palop, J. J., & Mucke, L. (2016). Network abnormalities and interneuron dysfunction in Alzheimer disease. *Nature Reviews. Neuroscience*, 17(12), 777–792. <https://doi.org/10.1038/nrn.2016.141>
- Papp, N., & Ktonas, P. (1977). Critical evaluation of complex demodulation techniques for the quantification of bioelectrical activity. *Biomedical Sciences Instrumentation*, 13, 135–145.
- Park, Y., Lee, K., Park, J., Bae, J. B., Kim, S.-S., Kim, D.-W., Woo, S. J., Yoo, S., & Kim, K. W. (2022). Optimal flickering light stimulation for entraining gamma rhythms in older adults. *Scientific Reports*, 12(1), 15550. <https://doi.org/10.1038/s41598-022-19464-2>
- Pastor, M. A., Artieda, J., Arbizu, J., Valencia, M., & Masdeu, J. C. (2003). Human cerebral activation during steady-state visual-evoked responses. *Journal of Neuroscience*, 23(37), 11621–11627. <https://doi.org/10.1523/JNEUROSCI.23-37-11621.2003>
- Pastor, M. A., Valencia, M., Artieda, J., Alegre, M., & Masdeu, J. C. (2007). Topography of cortical activation differs for fundamental and harmonic frequencies of the steady-state visual-evoked responses. An EEG and PET H215O study. *Cerebral Cortex*, (New York, N.Y.: 1991), 17(8), 1899–1905. <https://doi.org/10.1093/cercor/bhl098>
- Pfurtscheller, G., & Lopes da Silva, F. H. (1999). Event-related EEG/MEG synchronization and desynchronization: Basic principles. *Clinical Neurophysiology*, 110(11), 1842–1857. [https://doi.org/10.1016/S1388-2457\(99\)00141-8](https://doi.org/10.1016/S1388-2457(99)00141-8)
- Pfurtscheller, G., Stancák, A., & Neuper, Ch. (1996). Event-related synchronization (ERS) in the alpha band – an electrophysiological correlate of cortical idling: A review. *International Journal of Psychophysiology*, 24 (1), 39–46. [https://doi.org/10.1016/S0167-8760\(96\)00066-9](https://doi.org/10.1016/S0167-8760(96)00066-9)
- Pinheiro, J., & Bates, D. (2000). Mixed-Effects Models in S and S-PLUS. Springer-Verlag. <https://doi.org/10.1007/b98882>
- Pinheiro, J., Bates, D., DebRoy, S., Sarkar, D., & Team, R. C. (2022). Linear and nonlinear mixed effects models. R Package Version.



- Poline, J.-B., Worsley, K. J., Holmes, A. P., Frackowiak, R. S. J., & Friston, K. J. (1995). Estimating smoothness in statistical parametric maps: Variability of p values. *Journal of Computer Assisted Tomography*, 19(5), 788–796.
- Rauschel, V., Ruscheweyh, R., Krafczyk, S., & Straube, A. (2016). Test-retest reliability of visual-evoked potential habituation. *Cephalalgia*, 36(9), 831–839. <https://doi.org/10.1177/0333102415613613>
- Regan, D. (1989). *Human brain electrophysiology*. Elsevier.
- Rissman, R. A., De Blas, A. L., & Armstrong, D. M. (2007). GABA (a) receptors in aging and Alzheimer's disease. *Journal of Neurochemistry*, 103(4), 1285–1292. <https://doi.org/10.1111/j.1471-4159.2007.04832.x>
- Rissman, R. A., & Mobley, W. C. (2011). Implications for treatment: GABAA receptors in aging, down syndrome and Alzheimer's disease. *Journal of Neurochemistry*, 117(4), 613–622. <https://doi.org/10.1111/j.1471-4159.2011.07237.x>
- Rossion, B. (2014). Understanding face perception by means of human electrophysiology. *Trends in Cognitive Sciences*, 18(6), 310–318. <https://doi.org/10.1016/j.tics.2014.02.013>
- Schoenen, J. (1996). Deficient habituation of evoked cortical potentials in migraine: A link between brain biology, behavior and trigeminovascular activation? *Biomedicine & Pharmacotherapy*, 50(2), 71–78. [https://doi.org/10.1016/0753-3322\(96\)84716-0](https://doi.org/10.1016/0753-3322(96)84716-0)
- Schoffelen, J.-M., & Gross, J. (2009). Source connectivity analysis with MEG and EEG. *Human Brain Mapping*, 30(6), 1857–1865. <https://doi.org/10.1002/hbm.20745>
- Schupp, H. T., Stockburger, J., Codispoti, M., Junghöfer, M., Weike, A. I., & Hamm, A. O. (2006). Stimulus novelty and emotion perception: The near absence of habituation in the visual cortex. *Neuroreport*, 17(4), 365–369. <https://doi.org/10.1097/01.wnr.0000203355.88061.c6>
- Shibata, K., Yamane, K., Otuka, K., & Iwata, M. (2008). Abnormal visual processing in migraine with aura: A study of steady-state visual evoked potentials. *Journal of the Neurological Sciences*, 271(1–2), 119–126. <https://doi.org/10.1016/j.jns.2008.04.004>
- Spooner, R. K., Arif, Y., Taylor, B. K., & Wilson, T. W. (2021). Movement-related gamma synchrony differentially predicts behavior in the presence of visual interference across the lifespan. *Cerebral Cortex*, (New York, N.Y.: 1991), 31(11), 5056–5066. <https://doi.org/10.1093/cercor/bhab141>
- Spooner, R. K., Wiesman, A. I., Mills, M. S., O'Neill, J., Robertson, K. R., Fox, H. S., Swindells, S., & Wilson, T. W. (2018). Aberrant oscillatory dynamics during somatosensory processing in HIV-infected adults. *NeuroImage: Clinical*, 20, 85–91. <https://doi.org/10.1016/j.nicl.2018.07.009>
- Spooner, R. K., Wiesman, A. I., O'Neill, J., Schantell, M. D., Fox, H. S., Swindells, S., & Wilson, T. W. (2020). Prefrontal gating of sensory input differentiates cognitively impaired and unimpaired aging adults with HIV. *Brain Communications*, 2(2), fcaa080. <https://doi.org/10.1093/braincomms/fcaa080>
- Springer, S. D., Wiesman, A. I., May, P. E., Schantell, M., Johnson, H. J., Willett, M. P., Castelblanco, C. A., Eastman, J. A., Christopher-Hayes, N. J., Wolfson, S. L., Johnson, C. M., Murman, D. L., & Wilson, T. W. (2022). Altered visual entrainment in patients with Alzheimer's disease: Magnetoencephalography evidence. *Brain Communications*, 4(4), fcac198. <https://doi.org/10.1093/braincomms/fcac198>
- Sprugnoli, G., Munsch, F., Cappon, D., Paciorek, R., Maccone, J., Connor, A., El Fakhri, G., Salvador, R., Ruffini, G., Donohoe, K., Shafi, M. M., Press, D., Alsop, D. C., Pascual Leone, A., & Santarnecchi, E. (2021). Impact of multisection 40Hz tACS on hippocampal perfusion in patients with Alzheimer's disease. *Alzheimer's Research & Therapy*, 13(1), 203. <https://doi.org/10.1186/s13195-021-00922-4>
- Stam, C. J., van Cappellen van Walsum, A. M., Pijnenburg, Y. A. L., Berendse, H. W., de Munck, J. C., Scheltens, P., & van Dijk, B. W. (2002). Generalized synchronization of MEG recordings in Alzheimer's disease: Evidence for involvement of the gamma band. *Journal of Clinical Neurophysiology: Official Publication of the American Electroencephalographic Society*, 19(6), 562–574. <https://doi.org/10.1097/00004691-200212000-00010>
- Styr, B., & Slutsky, I. (2018). Imbalance between firing homeostasis and synaptic plasticity drives early-phase Alzheimer's disease. *Nature Neuroscience*, 21(4), 463–473. <https://doi.org/10.1038/s41593-018-0080-x>
- Tallon-Baudry, C. (2009). The roles of gamma-band oscillatory synchrony in human visual cognition. *Frontiers in Bioscience (Landmark Edition)*, 14(1), 321–332. <https://doi.org/10.2741/3246>
- Tallon-Baudry, C., & Bertrand, O. (1999). Oscillatory gamma activity in humans and its role in object representation. *Trends in Cognitive Sciences*, 3(4), 151–162. [https://doi.org/10.1016/S1364-6613\(99\)01299-1](https://doi.org/10.1016/S1364-6613(99)01299-1)
- Taulu, S., & Simola, J. (2006). Spatiotemporal signal space separation method for rejecting nearby interference in MEG measurements. *Physics in Medicine and Biology*, 51(7), 1759–1768. <https://doi.org/10.1088/0031-9155/51/7/008>
- Thompson, R. F., & Spencer, W. A. (1966). Habituation: A model phenomenon for the study of neuronal substrates of behavior. *Psychological Review*, 73(1), 16–43. <https://doi.org/10.1037/h0022681>
- Traikapi, A., & Konstantinou, N. (2021). Gamma oscillations in Alzheimer's disease and their potential therapeutic role. *Frontiers in Systems Neuroscience*, 15, 782399. <https://doi.org/10.3389/fnsys.2021.782399>
- Trevarrow, M. P., Kurz, M. J., McDermott, T. J., Wiesman, A. I., Mills, M. S., Wang, Y.-P., Calhoun, V. D., Stephen, J. M., & Wilson, T. W. (2019). The developmental trajectory of sensorimotor cortical oscillations. *NeuroImage*, 184, 455–461. <https://doi.org/10.1016/j.neuroimage.2018.09.018>
- Uhlhaas, P. J., Pipa, G., Lima, B., Melloni, L., Neuenschwander, S., Nikolić, D., & Singer, W. (2009). Neural synchrony in cortical networks: History, concept and current status. *Frontiers in Integrative Neuroscience*, 3, 17. <https://doi.org/10.3389/fnint.2009.07.017.2009>
- Uhlhaas, P. J., & Singer, W. (2006). Neural synchrony in brain disorders: Relevance for cognitive dysfunctions and pathophysiology. *Neuron*, 52(1), 155–168. <https://doi.org/10.1016/j.neuron.2006.09.020>
- Uusitalo, M. A., & Ilmoniemi, R. J. (1997). Signal-space projection method for separating MEG or EEG into components. *Medical & Biological Engineering & Computing*, 35(2), 135–140. <https://doi.org/10.1007/BF02534144>
- Van Veen, B. D., van Dronkelen, W., Yuchtman, M., & Suzuki, A. (1997). Localization of brain electrical activity via linearly constrained minimum variance spatial filtering. *IEEE Transactions on Bio-Medical Engineering*, 44(9), 867–880. <https://doi.org/10.1109/10.623056>
- Vialatte, F.-B., Maurice, M., Dauwels, J., & Cichocki, A. (2010). Steady-state visually evoked potentials: Focus on essential paradigms and future perspectives. *Progress in Neurobiology*, 90(4), 418–438. <https://doi.org/10.1016/j.pneurobio.2009.11.005>
- Wiesman, A. I., Christopher-Hayes, N. J., Eastman, J. A., Heinrichs-Graham, E., & Wilson, T. W. (2021). Response certainty during bimanual movements reduces gamma oscillations in primary motor cortex. *NeuroImage*, 224, 117448. <https://doi.org/10.1016/j.neuroimage.2020.117448>
- Wiesman, A. I., Murman, D. L., May, P. E., Schantell, M., Losh, R. A., Johnson, H. J., Willett, M. P., Eastman, J. A., Christopher-Hayes, N. J., Knott, N. L., Houseman, L. L., Wolfson, S. L., Losh, K. L., Johnson, C. M., & Wilson, T. W. (2021). Spatio-spectral relationships between pathological neural dynamics and cognitive impairment along the Alzheimer's disease spectrum. *Alzheimer's & Dementia: Diagnosis, Assessment & Disease Monitoring*, 13(1), e12200. <https://doi.org/10.1002/dad2.12200>
- Wiesman, A. I., O'Neill, J., Mills, M. S., Robertson, K. R., Fox, H. S., Swindells, S., & Wilson, T. W. (2018). Aberrant occipital dynamics differentiate HIV-infected patients with and without cognitive impairment. *Brain*, 141(6), Article 6, 1678–1690. <https://doi.org/10.1093/brain/awy097>

- Wilson, T. W., Heinrichs-Graham, E., Proskovec, A. L., & McDermott, T. J. (2016). Neuroimaging with magnetoencephalography: A dynamic view of brain pathophysiology. *Translational Research*, 175, 17–36. <https://doi.org/10.1016/j.trsl.2016.01.007>
- Wilson, T. W., Lew, B. J., Spooner, R. K., Rezich, M. S., & Wiesman, A. I. (2019). Aberrant brain dynamics in NeuroHIV: Evidence from magnetoencephalographic (MEG) imaging. *Progress in Molecular Biology and Translational Science*, 165, 285–320. <https://doi.org/10.1016/bs.pmbts.2019.04.008>
- Wilson, T. W., McDermott, T. J., Mills, M. S., Coolidge, N. M., & Heinrichs-Graham, E. (2018). tDCS modulates visual gamma oscillations and basal alpha activity in occipital cortices: Evidence from MEG. *Cerebral Cortex*, 28(5), 1597–1609. <https://doi.org/10.1093/cercor/bhx055>
- Wilson, T. W., Rojas, D. C., Reite, M. L., Teale, P. D., & Rogers, S. J. (2007). Children and adolescents with autism exhibit reduced MEG steady-state gamma responses. *Biological Psychiatry*, 62(3), 192–197. <https://doi.org/10.1016/j.biopsych.2006.07.002>
- Wilson, T. W., Slason, E., Asherin, R., Kronberg, E., Teale, P. D., Reite, M. L., & Rojas, D. C. (2011). Abnormal gamma and Beta MEG activity during finger movements in early-onset psychosis. *Developmental Neuropsychology*, 36(5), 596–613. <https://doi.org/10.1080/87565641.2011.555573>
- Worsley, K. J., Marrett, S., Neelin, P., Vandal, A. C., Friston, K. J., & Evans, A. C. (1996). A unified statistical approach for determining significant signals in images of cerebral activation. *Human Brain Mapping*, 4(1), 58–73. [https://doi.org/10.1002/\(SICI\)1097-0193\(1996\)4:1<58::AID-HBM4>3.0.CO;2-O](https://doi.org/10.1002/(SICI)1097-0193(1996)4:1<58::AID-HBM4>3.0.CO;2-O)
- Zhou, D., Li, A., Li, X., Zhuang, W., Liang, Y., Zheng, C.-Y., Zheng, H., & Yuan, T.-F. (2022). Effects of 40 Hz transcranial alternating current stimulation (tACS) on cognitive functions of patients with Alzheimer's disease: A randomised, double-blind, sham-controlled clinical trial. *Journal of Neurology, Neurosurgery, and Psychiatry*, 93(5), 568–570. <https://doi.org/10.1136/jnnp-2021-326885>

**How to cite this article:** Petro, N. M., Webert, L. K., Springer, S. D., Okelberry, H. J., John, J. A., Horne, L. K., Glesinger, R., Rempe, M. P., & Wilson, T. W. (2024). Optimal gamma-band entrainment of visual cortex. *Human Brain Mapping*, 45(10), e26775. <https://doi.org/10.1002/hbm.26775>